Appl. Phys. A (2017) 123:138
DOI 10.1007/s00339-017-0760-5

Applied Physics A
Materials Science & Processing

Healing mechanism of nanocrack in nanocrystalline metals during creep process

Md. Meraj[1] · Snehanshu Pal[1]

Received: 30 October 2016 / Accepted: 1 January 2017 / Published online: 2 February 2017

Abstract Molecular dynamics (MD) simulation has been performed to demonstrate the fate of cracks present inside ultrafine-grained (grain size ~ 7 nm) nanocrystalline Ni specimen during creep deformation process. It is observed that internal nanocracks are healed within a few pico-seconds of initial part of creep process even if the constant applied load on the specimen is tensile in nature and acting normal to crack surface in the outward direction. This kind of crack-healing phenomenon can be accounted by the facts such as stress-driven grain boundary migration, grain boundary diffusion and amorphization of specimen as per results obtained from this MD simulation. This MD study also reveals that the presence of nanocrack inside ultrafine-grained NC Ni in fact slightly improves creep properties and such enhancement of the creep properties is intensified as the size of internal crack increases.

1 Introduction

Nanocrystalline (NC) metals have average grain size less than 100 nm [1, 2] and generally possess poor ductility; therefore NC materials undergo failure many times suddenly without undergoing substantial plastic deformation [3–6]. Presence of incipient cracks (i.e. disintegration or gaps in a material having size less than the critical size) inside nanocrystalline metal may worsen the scenario by further reducing the earlier plastic deformation [7]. Such types of incipient cracks usually become significant for potentially life-limiting material failure processes [8] and therefore understanding the healing possibilities during deformation process in highly necessary. According to the study carried out by Aramfard and Deng, crack healing is favoured by interaction between shear-coupled grain boundary motion (SCGBM) and crack at relatively high temperature [9]. In another study, Xu and Demkowicz have found that disclination generated by stress-driven grain boundary motion can heal the nanocrack during shear deformation [10]. Moreover, such types of elimination of internal defects like cracks have significant influence on ductility of nanocrystalline metals. Therefore, understanding possibility and mechanisms responsible for healing of nanocracks during deformation process is essential. Presence of crack in NC materials creates internal free surface, which has significant influence on grain boundary motion as cooperative GB sliding and migration processes are observed to be taking place near free surfaces in case of NC materials [11]. However, several experimental [12–15] and simulation-based investigations [2, 7, 9–11, 16–18] have been carried out on the stress-driven grain boundary migration (SDGBM) and its effects on failure of materials, critical discussion on the role of SDGBM towards crack healing during deformation at high temperature is still due. Furthermore, although molecular dynamics (MD) have been recently utilized to investigate creep behaviour of NC materials to reveal the underlying mechanisms of creep of NC materials [19–21], detailed study on the influence of pre-existing nanocrack on creep deformation behaviour of NC metals has not been reported in the literature so far. In this paper, healing process of nano-crack present in ultrafine-grained NC Ni during creep deformation and the influence of the presence of pre-existing nanocrack on creep behaviour will be discussed.

✉ Snehanshu Pal
pals@nitrkl.ac.in; snehanshu.pal@gmail.com

[1] Department of Metallurgical and Materials Engineering, National Institute of Technology Rourkela, Rourkela, Odisha 769008, India

2 Simulation detail

A cubic specimen of NC Ni containing 8 grains having random crystallographic orientations and average grain size of 7 nm is prepared for carrying out simulation by Voronoi construction [22] using Atomeye software [23]. Each simulation box dimension is 14 nm × 14 nm × 14 nm. The stress–strain curve of NC Ni obtained from simulated tensile test performed with 10^8 s^{-1} strain rate at 1309 K temperature and plot of calculated potential energy per atom vs. temperature for NC Ni are presented in Fig. 1a, b, respectively. It is observed that yield point of NC Ni at 1309 K temperature is 3.12 GPa and melting point of the nanocrystalline Ni is ~1719 K temperature. The total number of atoms in NC Ni, NC Ni with (4×3×3) nm^3 nanocrack, NC Ni with (8×3×3) nm^3 nanocrack and NC Ni with (12×3×3) nm^3 nanocrack are 254,188, 250,867, 247,530 and 244,198, respectively, while nanocracks of various dimensions are positioned in the middle of specimen (shown in Fig. 2a). Energy minimization and equilibration of specimens by the conjugate gradient method at temperature of 1309 K (i.e. 0.76 of melting point for NC Ni having 7 nm grain size) have been carried out. After that, specimens are subjected to uniaxial tensile loading along Y-direction [010] up till 1 GPa load (i.e. ~0.32 of yield point of the nanocrystalline Ni specimen at 1309 K temperature), and then specimens are allowed to deform under same load at constant 1309 K temperature. Time step is taken as 2 fs for both creep simulation and MSD calculation. Diffusivity of NC Ni, NC Ni with (4×3×3) nm^3 nanocrack, NC Ni with (8×3×3) nm^3 nanocrack and NC Ni with (12×3×3) nm^3 nanocrack specimens have been evaluated at 1309 K temperature based on calculated mean square displacement by MD simulation. All MD simulations are performed using LAMMPS software [24]. Embedded atomic method (EAM) potential developed by Mendelev et al. [25] is used to perform all the simulations.

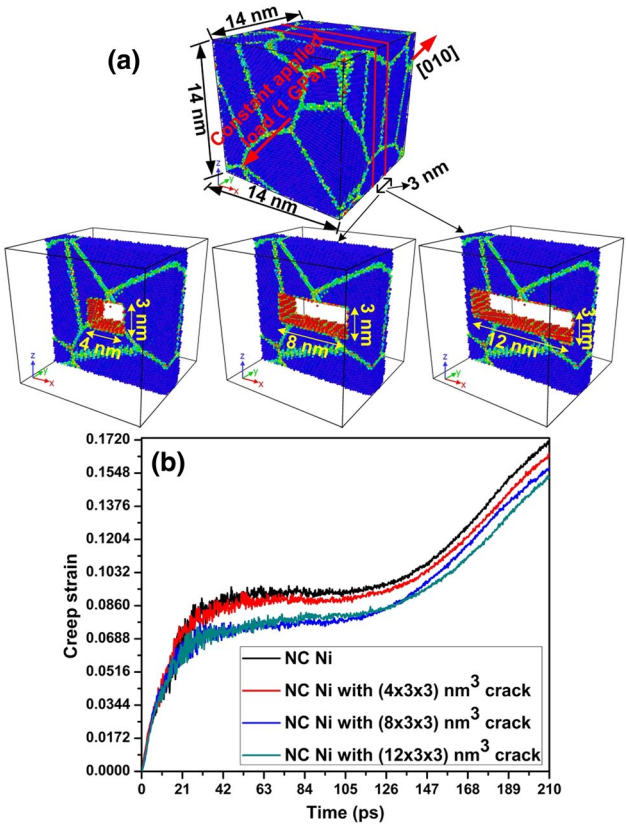

Fig. 2 **a** Initial atomic snapshot of complete NC Ni specimen and sectional view of NC Ni specimen showing internal nanocracks of different sizes and **b** creep curves of NC Ni having nanocracks of different sizes at 1309 K temperature and 1 GPa stress

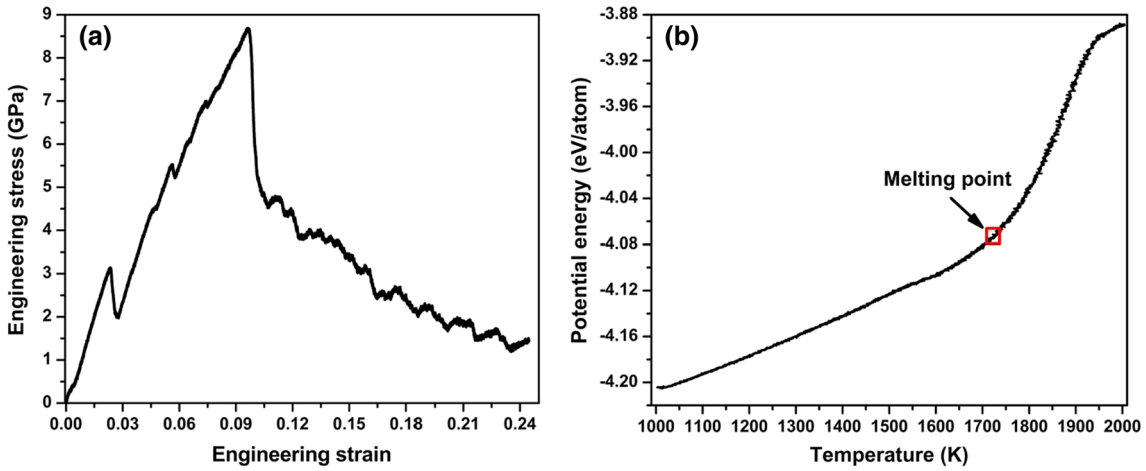

Fig. 1 **a** Plot of engineering stress–strain of nanocrystalline Ni specimen at 1309 K temperature and **b** plot of potential energy per atom vs. temperature for NC Ni having 7 nm average grain sizes to determine the melting point of NC Ni

Centro-Symmetry Parameter (CSP) is used to characterize the amount of inversion symmetry destroyed in regard to each atom's local environment at the time of creep deformation process [26]. Zero value of CSP indicates perfect specimen and positive value for specimen having defects. Atomic configuration snapshots coloured by CSP values have been prepared with the help of OVITO software [27].

3 Results and discussion

Influence of pre-existing internal nanocrack on creep behaviour of NC Ni and the healing of nanocrack during creep process along with its underlying mechanism have been discussed here. Creep curves of NC Ni having internal nanocracks of different sizes along with creep curve of perfect NC Ni for constant 1 GPa applied load and 1309 K temperature are presented in Fig. 2b. It is known from the literature that the creep process for ultrafine-grained NC Ni is mainly controlled by grain boundary diffusion process as Coble creep mechanism is dominant [19]. This actually makes the creep deformation very fast for such NC metallic systems, which is also evident from Fig. 2b. This can be accounted by the fact that NC metals exhibit stronger atomic diffusibility at their grain boundaries compared to conventional poly-crystalline materials [28]. Creep curves of NC Ni having pre-existing internal nanocrack are observed to be shifted marginally towards lower creep strain in comparison with the creep curve of perfect NC Ni. This can be attributed to fact that diffusivity is slightly lesser for NC Ni having internal nanocrack compared to NC Ni having no crack, which is evident from the values of diffusivity presented in Table 1. Diffusivity before and after healing nanocrack is determined to study the influence of crack size on the diffusivity of sample during creep deformation along with the diffusivity after complete amorphization of sample (refer Table 1). Diffusivity immediately after nanocrack healing is observed to be slightly more for the specimen having larger nanocrack compared to the specimen having smaller nanocrack or no nanocrack. On the contrary, diffusivity after complete amorphization is found to be slightly less for the specimen having larger nanocrack in comparison with the specimen having smaller nanocrack. It is also worth of mentioning that the diffusivity is increased significantly after amorphization with respect to the stage just after nanocrack healing for all the cases studied here.

Atomic snapshots (coloured as per CSP values) showing different stages of nanocrack healing phenomenon taking place during tensile creep process are presented in Fig. 3. Significant variation in grain structure indicating the occurrence of grain boundary mobility due to stress is observed in these presented snapshots, which is also similar to findings reported in literature for room-temperature deformation of NC Ni having 5 nm average grain size [29]. Generation and movement of crystal defects are observed and some linear crystal defects among them binds the surface of the crack with main body of the specimen. These kinds of linear defects are known as disclination [30]. Furthermore, disclinations like stress-driven grain boundary migration are found to heal the nanocrack present in the NC Ni; similar observation is also reported for Ni bi-crystal by Xu et al. [10]. The grain boundary region is broadened as creep deformation process progresses; moreover, earlier initiation of this grain boundary widening phenomenon is observed near the nanocrack surface compared to other parts of the specimen (refer snap shots after 1 ps in Fig. 3). This is due to the gathering of atoms on the grain boundaries as resultant diffusion fluxes across the grain boundaries are there. Localized amorphization near nanocrack surface is seen at a very early stage and then amorphization of full specimen is found to be taking place. Healing of the internal nanocrack is also observed to be happening simultaneously, which is owing to the stress-induced grain boundary migration and grain boundary diffusion process. Schematic pictorial representation of nanocrack healing mechanism along with some atomic snapshots coloured according to CSP values (taking range 0–50 for better visualization) are shown in Fig. 4. To study the movement of atoms situated near or at the nanocrack surface region, atomic trajectories (denoted by yellow colour) of atoms selected among them (as marked by red colour in Fig. 4b, c at $t = 1$ ps) are shown in Fig. 4b, c for nanocracks having $(4 \times 3 \times 3)$ nm^3 and $(12 \times 3 \times 3)$ nm^3, respectively. Nanocrack is observed

Table 1 Diffusion coefficient of NC Ni having nanocracks of different sizes

Name of sample	Diffusion coefficient (m^2/s) $\times 10^{-10}$		
	Initial specimen (before crack healing)	Just after crack healing	Complete amorphous specimen
NC Ni	2.62	–	–
NC Ni with $(4 \times 3 \times 3)$ nm^3 crack	2.12	1.56	85.54
NC Ni with $(8 \times 3 \times 3)$ nm^3 crack	2.01	2.21	84.67
NC Ni with $(12 \times 3 \times 3)$ nm^3 crack	1.55	2.44	83.90

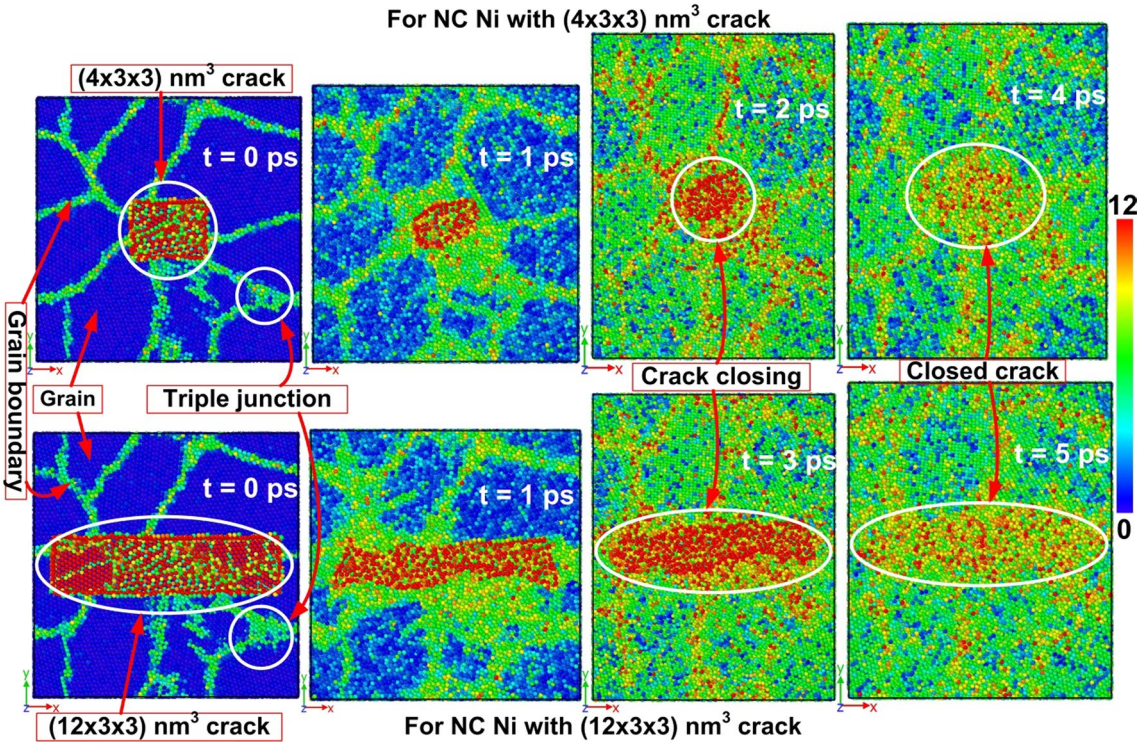

Fig. 3 Atomic configuration snapshots for NC Ni with (4×3×3) nm^3 nanocrack and NC Ni with (12×3×3) nm^3 nanocrack at different time steps

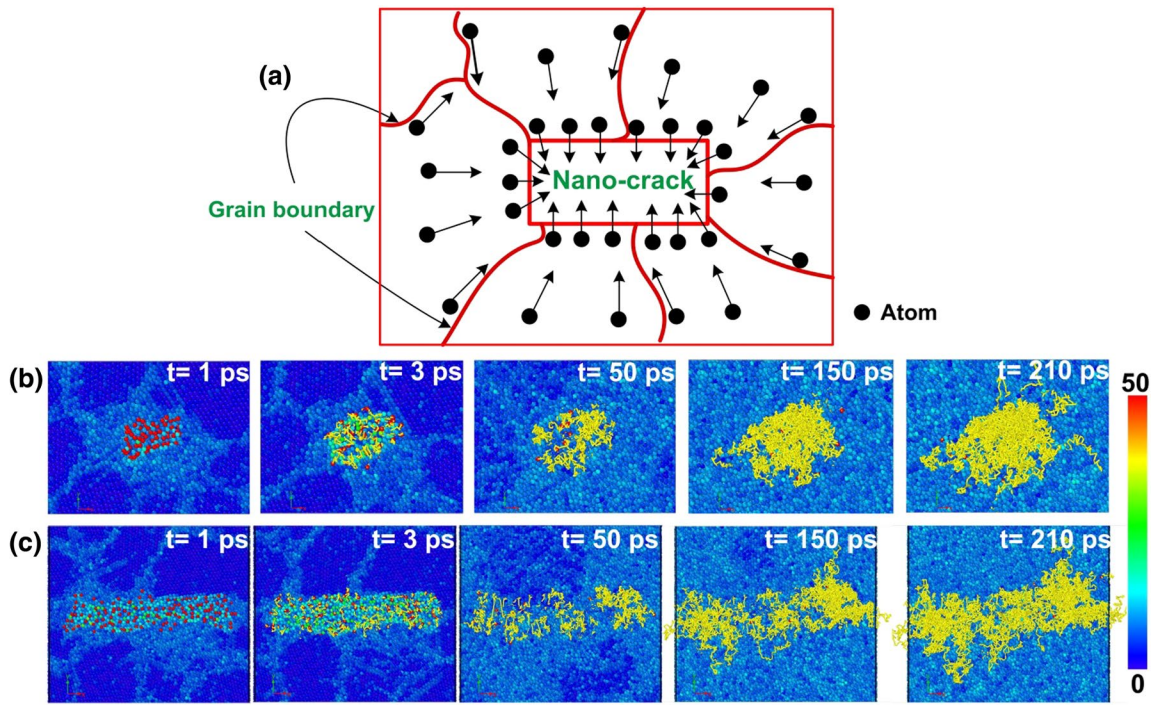

Fig. 4 **a** Schematic pictorial representation of nanocrack healing mechanism and simulated atomic trajectory snapshots of NC Ni having (**b**) (4×3×3) nm^3 and **c** (12×3×3) nm^3 nanocrack at different time steps (*red* colour represents the selected atoms and *yellow* colour represents the atomic trajectory)

to be healed by the movement of atoms present near or at the nanocrack surface, and nearby grain boundaries as per traced atomic trajectory lines. It is revealed from Fig. 4 that atoms present at or near nanocrack surface and grain boundaries nearby the nanocrack surface move towards the hollow region of the nanocrack region. This actually leads to the healing of the nanocrack with the progress of creep deformation. Nanocrack healing occurred slightly earlier in case of NC Ni with (4×3×3) nm^3 crack compared to NC Ni with (12×3×3) nm^3 crack, as evident from Fig. 3. Hence, it can be inferred that surface diffusion process as well as grain boundary diffusion near the nanocrack are significant factors for crack healing during creep deformation in the case of NC Ni. It is also found in Fig. 5 that atomic diffusivity becomes more in case of region nearer to nanocrack with respect to the region farther from nanocrack for NC Ni having (4×3×3) nm^3 nanocrack taken as a representative case. This leads to faster closing of nanocrack during creep process and also causes faster amorphization in the region near the nanocrack. NC Ni specimen having (12×3×3) nm^3 nanocrack has also been equilibrated at 1309 K temperature for 210 ps time duration to understand the contribution of temperature on nanocrack healing if at all is there. The corresponding atomic snapshots (coloured as per CSP values) after different time periods are shown in Fig. 6. It is found that healing of the nanocrack has not happened in this case. Only slight reduction in nanocrack size near 210 ps time is observed when the specimen is subjected to zero load at 1309 K temperature. In addition, creep deformation simulations of NC Ni specimen having (12×3×3) nm^3 nanocrack have been carried out under constant 0.1 GPa applied load for 300 and 500 K temperatures to check the crack healing behaviour in case of lower stress and temperature condition and relevant atomic configuration snapshots are given in Figs. 7 and 8, respectively. Nanocrack healing time is found to be almost equal for the

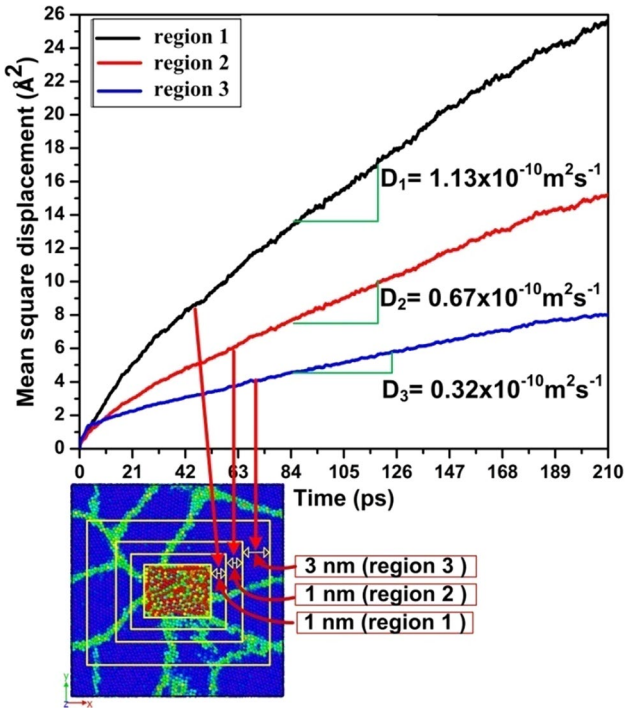

Fig. 5 Mean square displacement vs. time plots of NC Ni with (4×3×3) nm^3nanocrack at three different regions

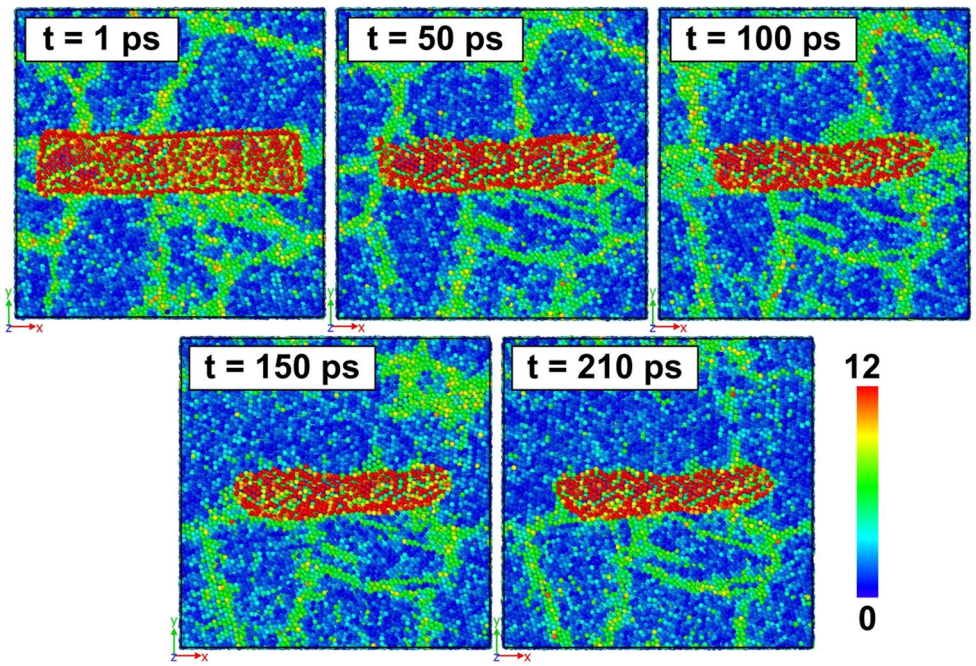

Fig. 6 Atomic configuration snapshots for NC Ni with (12×3×3) nm^3 nanocrack with zero applied load and 1309 K temperature at different time steps

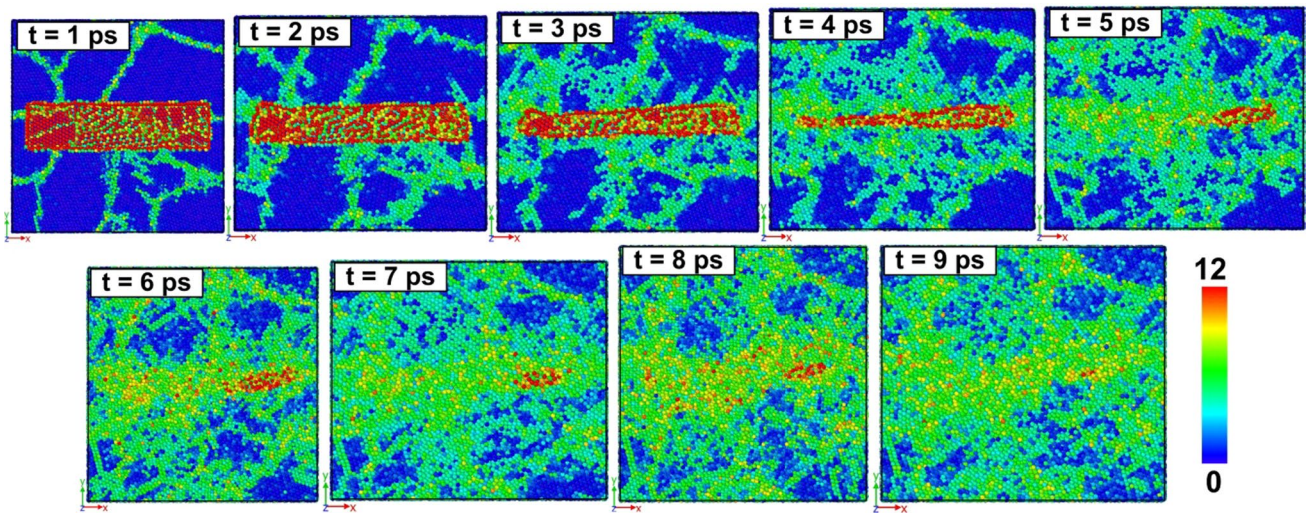

Fig. 7 Atomic configuration snapshots for NC Ni with (12×3×3) nm^3 nanocrack under constant lower stress (i.e. 0.1 GPa) and temperature (i.e. 300 K) at different time steps

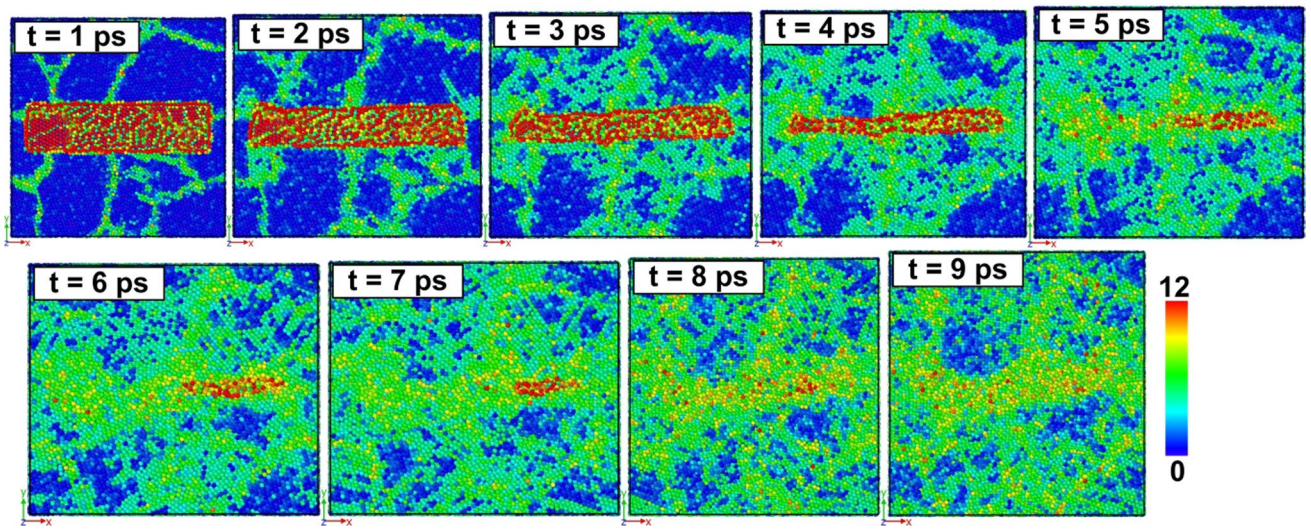

Fig. 8 Atomic configuration snapshots for NC Ni with (12×3×3) nm^3 nanocrack under constant lower stress (i.e. 0.1 GPa) and 500 K temperature at different time steps

cases having variation in creep temperatures (e.g. 300 and 500 K) if the applied load is taken same for each simulation case. Applied stress is found to be a major and dominant contributory factor for crack healing process during creep compared to creep temperature.

4 Conclusions

The MD simulation results show that quick healing of pre-existing internal nanocrack is taking place during creep process of ultrafine-grained (grain size ~ 7 nm) NC Ni. Stress-driven grain boundary migration and grain boundary diffusion are found to be contributory factors for such healing phenomenon of the nanocrack. It is also observed from this study that internal nanocrack slightly enhances the creep resistance of ultrafine-grained NC Ni.

Acknowledgements Authors are thankful to Mrs. Debanjana Bhattacharyya for checking the language and proof of the manuscript.

References

1. H. Gleiter, Acta mater **48**, 1 (2000)
2. J. Schiøtz, K.W. Jacobsen, Science **301**, 1357 (2003)

3. J.A. Sharon, H.A. Padilla, B.L. Boyce, J. Mater. Res. **28**, 1539 (2013)
4. A.Y. Chen, Y.K. Li, J.B. Zhang, D. Pan, J. Lu, Mater. Des **47**, 316 (2013)
5. M. Dao, L. Lu, R.J. Asaro, J.T.M. De Hosson, E. Ma, Acta Mater **55**, 4041 (2007)
6. Z.F. Liu, Z.H. Zhang, J.F. Lu, A.V. Korznikov, E. Korznikova, F.C. Wang, Mater. Des **64**, 625 (2014)
7. G. Xu, M.J. Demkowicz, Extreme Mech. Lett. (2016). doi:10.1016/j.eml.2016.03.011
8. L. Ma, S. Xiao, H. Deng, W. Hu, Appl. Phys. A **118**, 1399 (2015)
9. M. Aramfard, C. Deng, J. Appl. Phys **119**, 085308 (2016)
10. G.Q. Xu, M.J. Demkowicz, Phys. Rev. Lett. **111**, 145501 (2013)
11. I.A. Ovid'ko, A.G. Sheinerman, Acta Mater **121**, 117 (2016)
12. T.J. Rupert, D. S. Gianola, Y. Gan, K.J. Hemker, Science **326**, 1686 (2009)
13. B. Beausir, C. Fressengeas, Int. J. Solids Struct. **50**, 137 (2013)
14. M. Legros, D.S. Gianola, K.J. Hemker, Acta Mater **56**, 3380 (2008)
15. F. Mompiou, M. Legros, A. Boé, M. Coulombier, J.P. Raskin, T. Pardoen, Acta Mater **61**, 205 (2013)
16. Z.T. Trautt, A. Adland, A. Karma, Y. Mishin, Acta Mater **60**, 6528 (2012)
17. D. Farkas, S. Mohanty, J. Monk, Mater. Sci. Eng. A **493**, 33 (2008)
18. J. Schiøtz, F.D. Di Tolla, K.W. Jacobsen, Nature **391**, 561 (1998)
19. M. Meraj, N. Yedla, S. Pal, Mater. Lett **169**, 265 (2016)
20. S. Pal, M. Meraj, Mater. Des **108**, 168 (2016)
21. S. Pal, M. Meraj, C. Deng, Comput. Mater. Sci. **126**, 382 (2017)
22. D. Chen, Comput. Mater. Sci. **3**, 327 (1995)
23. J. Li, Modell. Simul. Mater. Sci. Eng. **11**, 173 (2003)
24. S. Plimpton, J. Comput. Phys **117**, 1 (1995)
25. M.I. Mendelev, M.J. Kramer, S.G. Hao, K.M. Ho, C.Z. Wang, Philos. Mag. **92**, 4454 (2012)
26. C.L. Kelchner, S.J. Plimpton, J.C. Hamilton, Phys. Rev. B **58**, 11085 (1998)
27. A. Stukowski, Modell. Simul. Mater. Sci. Eng. **18**, 015012 (2009)
28. J.C.M. Li, Mechanical properties of nanocrystalline materials, (CRC Press, Boca Raton, 2011)
29. D. Farkas, A. Frøseth, H. Van Swygenhoven, Scr. Mater **55**, 695 (2006)
30. A.E. Romanov, Eur. J. Mech. A/Solids **22**, 727 (2003)